PROCEEDINGS OF SCIENCE

Topological features of the deconfinement transition in the SU(3) Yang-Mills theory

Réka Á. Vig,[a,*] **Szabolcs Borsányi,**[a] **Zoltán Fodor,**[a,b,c,d] **Daniel Godzieba,**[b] **Ruben Kara,**[a] **Paolo Parotto**[b] **and Dénes Sexty**[e]

[a] *University of Wuppertal, Department of Physics, Wuppertal D-42119, Germany*
[b] *Pennsylvania State University, Department of Physics, University Park, PA 16802, USA*
[c] *Inst. for Theoretical Physics, ELTE Eötvös Loránd University, Pázmány P. sétány 1/A, H-1117 Budapest, Hungary*
[d] *Jülich Supercomputing Centre, Forschungszentrum Jülich, D-52425 Jülich, Germany*
[e] *University of Graz, NAWI Graz, Institute for Physics, A-8010 Graz, Austria*
E-mail: revig@uni-wuppertal.de, borsanyi@uni-wuppertal.de, fodor@bodri.elte.hu, dag5611@psu.edu, rkara@uni-wuppertal.de, paolo.parotto@gmail.com, denes.sexty@uni-graz.at

The QCD crossover is marked by the rapid change in various observables such as the chiral condensate, the Polyakov loop or the topological susceptibility. We studied the topological properties in pure SU(3) gauge theory where the transition is first order. Our study focused on the topological susceptibility and the b_2 coefficient of the expansion of the free energy density around $\theta = 0$. There was already some evidence for the discontinuity in the topological susceptibility at the transition temperature in SU(N) Yang-Mills theories. We determined the continuum extrapolated value of this discontinuity for $N = 3$ in the infinite volume limit. We also determined the temperature dependence of the b_2 coefficient at $\theta = 0$.

The 39th International Symposium on Lattice Field Theory (Lattice2022),
8-13 August, 2022,
Rheinische Friedrich-Wilhelms-Universität Bonn, Bonn, Germany

*Speaker

PoS(LATTICE2022)194

1. Introduction

The high temperature cross-over in quantum chromodynamics (QCD) is a highly investigated topic in theoretical physics and particularly in the lattice community. In the cross-over region deconfinement of the strongly interacting matter is accompanied by several other phenomena like the restoration of the approximate chiral symmetry, localization of the lowest Dirac eigenmodes and a rapid change in the fluctuations of the topological charge Q. The latter can be observed through the topological susceptibility

$$\chi = \frac{\langle Q^2 \rangle}{V_4} \tag{1}$$

where V_4 is the Euclidean four-volume and Q is the topological charge, defined in the continuum theory as

$$Q = \frac{1}{32\pi^2} \int_{V_4} d^4x \mathrm{Tr}\, \epsilon_{\mu\nu\rho\sigma} F_{\mu\nu} F_{\rho\sigma} \ . \tag{2}$$

The quick suppression of topological fluctuations in the transition region is supported analitically by a perturbative study of instantons [1]. This behavior of χ was observed in several studies on the lattice [2–4].

In pure SU(3) Yang-Mills theory, in contrast to full QCD deconfinement is a genuine first order phase transition. It was shown also in this case that χ falls sharply at the transition temperature [5]. On top of this in Ref. [6] it was pointed out on ensembles with four volume $V_4 = 32^3 \times 5$ that χ differs in the hot and cold phases at $T = T_c$. Considering these results we assume that the function $\chi(T)$ has a discontinuity $\Delta\chi$ at the transition temperature which we aimed to calculate in the continuum and infinite volume limit. We discuss our results in Sec. 4.

The value of $\Delta\chi$ can be estimated in the following way. As the topological susceptibility appears in the Taylor expansion of the thermodynamic potential with respect to the CP-breaking θ parameter, we can expect, that the behaviour of χ at the transition is linked to the details of the phase diagram in the $T - \theta$ plane. According to Refs. [7, 8] in the case of a first order transition the curvature parameter R_θ, defined as

$$\frac{T_c(\theta)}{T_c(0)} = 1 + R_\theta \theta^2 + O(\theta^4) \tag{3}$$

is related to the latent heat $\Delta\epsilon$ and the discontinuity of the topological susceptibility

$$\Delta\chi = 2\Delta\epsilon R_\theta \ . \tag{4}$$

The curvature was determined in Ref. [7, 8] to be $R_\theta = -0.0178(5)$ by using imaginary θ simulations. Combining this with recent result of the latent heat $\Delta\epsilon/T_c^4 = 1.025(21)(27)$ determined in a precision study [9] we arriwe to an estimate of the discontinuity $\Delta\chi/T_c^4 = -0.0365(18)$.

Besides χ higher moments of the topological chage distribution $P(Q)$ are also related to Taylor coefficients of the free energy density. The kurtosis of $P(Q)$ can be studied through the b_2 coefficient

$$b_2(T) = -\frac{\chi_4(T)}{12\chi(T)}, \qquad \chi_4 = \frac{1}{\mathcal{V}} \left[\langle Q^4 \rangle - 3 \langle Q^2 \rangle^2 \right] \ . \tag{5}$$

Studying $b_2(T)$ at the transition region was proved useful as its value is related the structure of the topological fluctuations. At low temperatures gauge fluctuations in pure SU(3) gauge theory

are described by the instanton liquid model [10] whereas in the high temperature phase lumps of charge become sparse and can be described by the dilute instanton gas approximation (DIGA). It was shown that DIGA is an accurate description at temperatures as close to T_c as $1.045T_c$ and $1.15T_c$ [11, 12]. In this case the interaction between topological objects can be neglected which means that $P(Q)$ is Skellam distribution [11]. Using this to calculate charge averages in Eq. 5 yealds to the analytical value of $b_2 = -1/12$. At $T = 0$ empirical results on the lattice indicate that $b_2 \approx -0.02$ [13–17], and does not depart much from this value for $T < T_c$. Thus examining the function $b_2(T)$ accross the transition one can see when it departs from this empirical value and how fast it approaches the DIGA limit. Our lattice results for $b_2(T)$ and $\chi(T)$ are discussed in Sec. 3 after a brief introduction of the setup of lattice simulations in Sec. 2. Finally we summarize our results in Sec. 5 and conclude.

2. Simulation details

We simulated pure SU(3) lattice gauge theory with the Symanzik improved gauge action. Gauge ensembles were generated in the vicinity of the transition point with several gauge coupling values using parallel tempering (for a detailed descripcion see [9]). We stored those configurations that were generated at the crtical coupling that set with a precision of $10^{-3}\frac{T}{T_c}$. In Tab. 1 we show the number of stored configurations corresponding to lattices with different spatial volume and temporal extent. We measured the Symanzik improved topological charge [18–20] on each gauge

		N_t				
		6	7	8	10	12
	4	497478	64901	77902	40054	20604
	4.5	-	-	30544	-	-
LT	5	20041	6524	36610	13473	-
	6	67185	7875	53325	24475	-
	8	30581	6677	7372	-	-

Table 1: Number of gauge configurations generated at the transition point β_c. LT means the aspect ratio and N_t is the temporal extension in lattice units.

configuration:

$$Q = \sum_{mn\in\{11,12\}} c_{nm} Q_{mn} \quad \texttt{with} \quad c_{11} = 10/3, \quad c_{12} = -1/3 \tag{6}$$

$$\text{and} \quad Q_{mn} = \frac{1}{32\pi^2}\frac{1}{m^2n^2}\sum_x \sum_{\mu,\nu,\rho,\sigma} \epsilon_{\mu\nu\rho\sigma} Tr(\hat{F}_{\mu\nu}(x;m,n)\hat{F}_{\rho\sigma}(x;m,n)), \tag{7}$$

where the $\hat{F}_{\mu\nu}(x;m,n)$ quantity is defined as the average of clover terms built from $m \times n$ plaquets in the $\mu\nu$ plane and centered at the lattice site x. We show a visual representation of $\hat{F}_{\mu\nu}(x;m,n)$ in Fig. 1. In later analysis we used the renormalized topological charge which we obtained by introducing smearing on the gauge field via the Wilson flow [21]. The computational cost of calculating the Wilson flow increases with the flow time t, thus we had to compromise when we

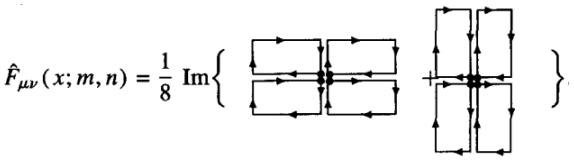

Figure 1: An illustration from [19] of $\hat{F}_{\mu\nu}(x;m,n)$ showing that it is built from the average of clover terms with $n \times m$ plaquets.

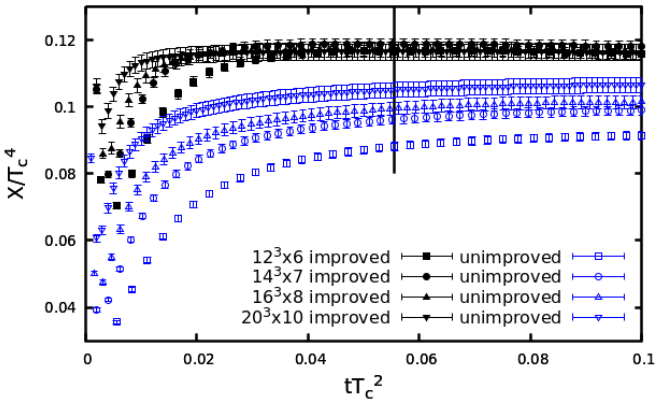

Figure 2: Topological susceptibility calculated on lattices of aspect ratio LT=2 with different resolutions. Data represented with filled points (of color black) are determined from the Symanzik-improved topological charge compared to unimproved data shown as empty points (of color blue).

chose t so that it is small but large enough reduce the effects of finite lattice spacings. In practice we analysed the dependency of χ on the normalized flow time tT_c^2 for lattices of aspect ratio $LT = 2$ which we show in Fig. 2. Results with different lattice spacings can be compared by using the normalized topological susceptibilty $\chi/T_c^4 = (T/T_c)^4 \langle Q \rangle (N_t^4/V_4)$, thus in the figures we show this quantity from now on. Our choice is $tT_c^2 = 1/16$ (indicated with a black vertical line) which falls in the plateau region even for the coarsest lattice. Filled points (of black color) show results calculated using the Symanzik-improved Q and as a comparison we also show data calculated using the unimproved Q represented by empty points (of color blue).

Besides simulations at the transition point we also generated ensembles in the vicinity of the transition $0.9\ T_c < T < 1.1\ T_c$ by employing parallel tempering. In this case we measured Q at not only one but several temperatures thus to reduce computational costs we used stout smearing instead of the Wilson flow as we kept the same physical smearing radius. This means that we performed a number of stout smearings with $\rho = 0.125$. We chose a number of smearing steps such that $t/T_c^2 = 1/18 = N_{\text{smear}}\rho/N_t^2$, which means $N_{\text{smear}} = 16$ for the coarsest lattice ($N_\tau = 6$) and $21.\bar{7}$ steps for $N_\tau = 7$, $28.\bar{4}$ for $N_\tau = 8$, and $44.\bar{4}$ steps for $N_\tau = 10$. As there are non integer steps we determined Q through interpolation in these cases. In Tab. 2 we show topological susceptibilities calculated from lattices of $LT = 2$ by using both definitions of the renormalized charge. There is a precise agreement in the results of the two different methods and the differences are much smaller than the statistical error, therefore in further analyzis we neglect the systematic error coming from the different renormalization methods.

	χ/T_c^4	
N_t	Wilson flow	stout smearing
6	0.11702(156)	0.11718(155)
7	0.11882(176)	0.11884(176)
8	0.11720(231)	0.11722(233)
10	0.11652(248)	0.11655(248)
12	0.11416(311)	0.11413(311)

Table 2: Topological susceptibility calculated at $t/T_c^2 = 1/16$ at temporal extents $N_t = 6, 7, 8, 10, 12$ via the Wilson flow (second column) compared to χ calculated after stout smearing steps (third column) corresponding to the same physical flow time.

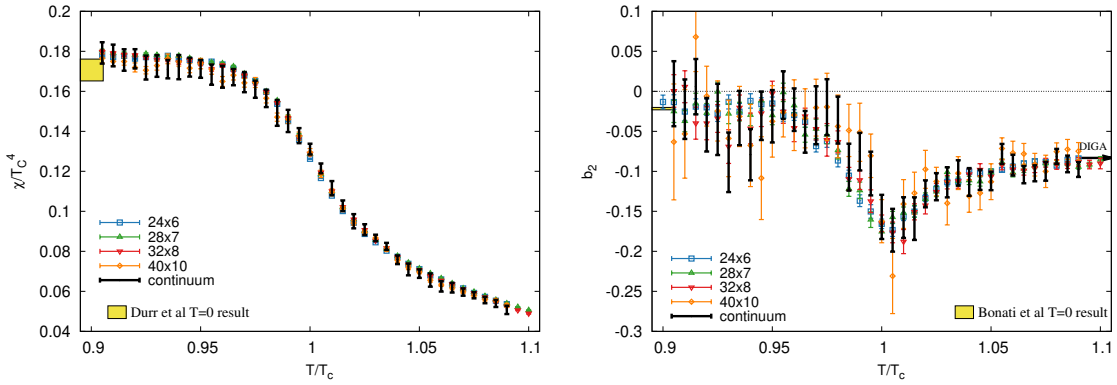

Figure 3: The topological susceptibility (left) and b_2 coefficient (right) as functions of the normalized temperature. Results for lattices with physical volume $LT = 4$ and $N_t = 6, 7, 8, 10$ are shown in blue, green, red and orange respectively. The continuum extrapolation, which includes statistical and systematic uncertainties, is shown in black.

3. The susceptibility and $b_2(T)$ in the transition region

We examined the temperature dependence of the quantities b_2 and χ in temperature range $0.9T_c < T < 1.1T_c$. In fig. 3 we show our results for the topological susceptibility χ (left) and the coefficient b_2 (right) for the aspect ratio $LT = 4$. The colored points correspond to lattices with $N_t = 6, 7, 8, 10$. We carried out a continuum extrapolation for these curves that we show with black in the figure. The continuum extrapolation was done in the following way. We first interpolated the different curves in β with a cubic spline, then we divided the horizontal axis evenly and performed the continuum extrapolation at each of these temperatures.

For the topological susceptibility we estimated the statistical errors of the continuum extrapolation by first fitting on the full data including $N_t = 6$ lattices then excluding them in a second fit. The statistical errors on the $b_2(T)$ result on the finest lattice ($40^3 \times 10$) is too large for this estimation for b_2; there all four lattices were included in the continuum limit. In Fig. 3 we also show the corresponding $T = 0$ results for χ [22] and the $b_2(T = 0) = -0.0216(15)$ continuum result is from Ref. [13].

In Fig. 4 we show the volume dependence of results while we fixed the temporal extent to

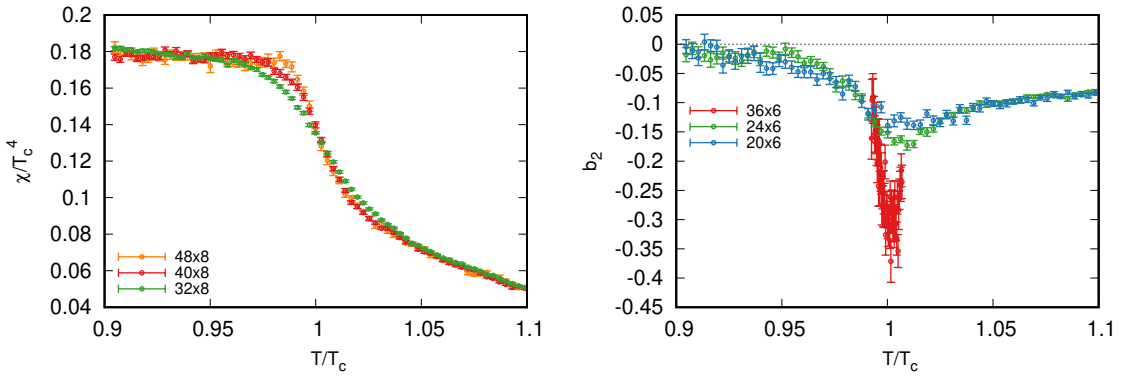

Figure 4: The topological susceptibility (left) at $N_t = 8$ and b_2 coefficient at $N_t = 6$ (right) as functions of the normalized temperature. Results for lattices with different physical volumes are shown with different colors.

$N_t = 6$ and 8 in the case of b_2 (right panel) and χ (left panel) respectively. As we go closer to the infinite volume limit the slope of the $\chi(T)$ curve become steeper which is also an indication that a discontinuity is to be expected in the infinite volume case. We also see that by increasing the volume the dip of $b_2(T)$ at the transition become more pronounced. This can be understood by looking at the structure of the formula of b_2. At $T = T_c$ the statistical weight of the cold and hot phases are the same $w^{cold} = w^{hot} = 1/2$ and simple calculation yields to

$$b_2 = \frac{\chi^{cold} b_2^{cold} + \chi^{hot} b_2^{hot}}{\chi^{cold} + \chi^{hot}} + \frac{V_4}{16} \frac{\Delta\chi^2}{\bar{\chi}} \tag{8}$$

where b_2^{cold} and b_2^{hot} means the value of the coefficient b_2 when there are only configurations corresponding to the cold or hot phase, $\Delta\chi = \chi^{cold} - \chi^{hot}$ and $\bar{\chi} = \frac{1}{2}\chi^{cold} - \frac{1}{2}\chi^{hot}$. In the infinite volume limit the two phases coexist only at $T = T_c$ and b_2 would be a negative Dirac delta as the second term in Eq. 8 is proportional to the volume. In finite volume simulations the two phases coexist with different weight factors in the vicinity of the transition, that is why we see a dip with a finite width and depth in the right hand sides panels in Fig. 3 and Fig. 4. Further increasing the temperature only the hot phase configurations remain and $b_2(T)$ stabilizes at the prediction of the DIGA picture.

4. The discontinuity of the topological susceptibility

We showed in the previous section that $\chi(T)$ suddenly drops as we approach the transition temperature. In the thermodynamic limit we expect a discontinuity at $T = T_c$, thus in this section we focus on the transition point where both confined configurations with $Z(3)$ center symmetry and the deconfined configurations with spontaneously broken center symmetry are present with comparable statistical weights. The Polyakov-loop serves as an order parameter for deconfinement in the quenched theory, thus examining its spatial average $P = \frac{1}{N_x^3} \sum_x P(x)$, where N_x is the spatial extent of the lattice, allows us to identify which phase a given configuration belongs to. Finite volume histograms of the Polyakov-loop magniude $|P|$ have a double peak structure which we show

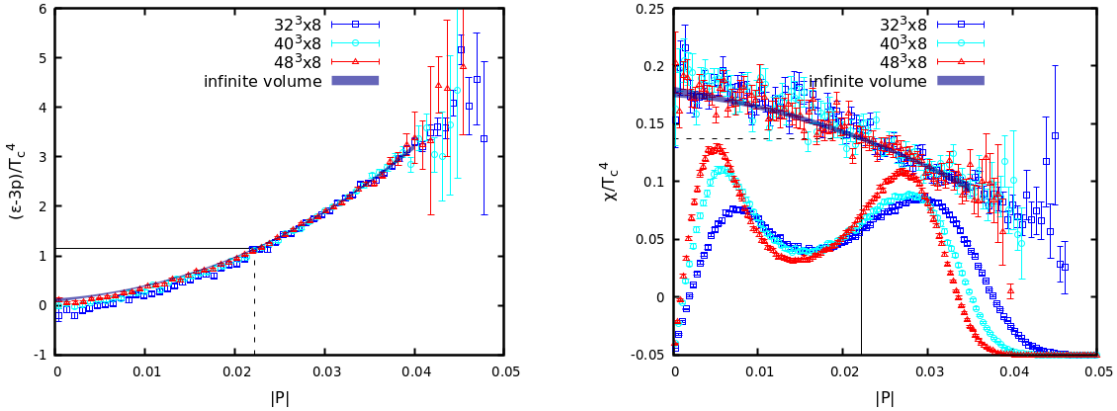

Figure 5: Discontinuity of χ at the transition temperature of ensembles listed in Tab. 1. Results of different lattices are projected onto the infinite volume plane (top) and the continuum plane (bottom). The blue bands are linear (three parameter) fits of the projected data using the same parameters as in the two dimensional fit.

in the right panel of Fig. 6 together with the topological susceptibility calculated in each bin of the histogram. We also determined the infinite volume limit of $\chi(|P|)$ via a two dimensional fit of a second degree polynomial. Considering the Polyakov-loop histogram in the infinite volume case instead of two peaks it would be a double Dirac delta one at $|P|^{cold} = 0$ and the other at some finite value of $|P|^{hot}$.

The hot phase value of the Polyakov-loop $|P|^{hot}$ can be determined by knowing the latent heat $\Delta\epsilon$. For this we have to examine the trace anomaly $(\epsilon - 3p)/T_c^4$ as a function of $|P|$. We show this in the left panel of Fig. 6 for $N_t = 8$ with its infinite volume limit which we determined by a two dimensional fit. The latent heat is the difference between trace anomaly's value at $|P| = 0$ and its value at $|P|^{hot}$. We can determine the latent heat using the same method as [9] at a fixed N_t. Adding this result to the trace anomaly the $|P| = 0$ (indicated with a solid horizolntal line) we can read the $|P|^{hot}$ value (which we indicate with dashed vertical line). Then we can obtain $\Delta\chi$ by simply subtracting $\chi(|P| = 0)$ from $\chi(|P|^{hot})$. We did this for different lattice resolutions but the statistical error in this case was higher compared to the direct calculation of $\Delta\chi$ which we discuss in the following.

We can determine $\Delta\chi$ directly for each finite volume ensemble by distinguishing configurations corresponding to the hot and cold phases. A natural way to do this is to cut Polyakov-loop histograms and at their minimum $|P_c|$ between the two peaks. Then we consider configurations with $|P| < |P_c|$ to be in the cold phase and those with $|P| > |P_c|$ to be in the hot phase. Then we can assign topological susceptibilities corresponding to both peaks and calculate $\Delta\chi$ by subtracting the value of χ in the cold phase from that of the hot phase. By calculating $\Delta\chi$ for each lattice ensemble we could extrapolate its continuum and infinite volume limit via a two dimensional fit. We illustrate this in Fig. 6 with a linear fit on the data. On the left panel of the figure we show data projected to the infinite volume plane and on the right panel data projected to the continuum plane together with error bands of the linear fit. The main result for the discontinuity of the topological susceptibility is

$$\Delta\chi/T_c^4 = -0.0344(44)(32) \tag{9}$$

with the statistical and systematic errors. The systematic error has two main sources. One is coming

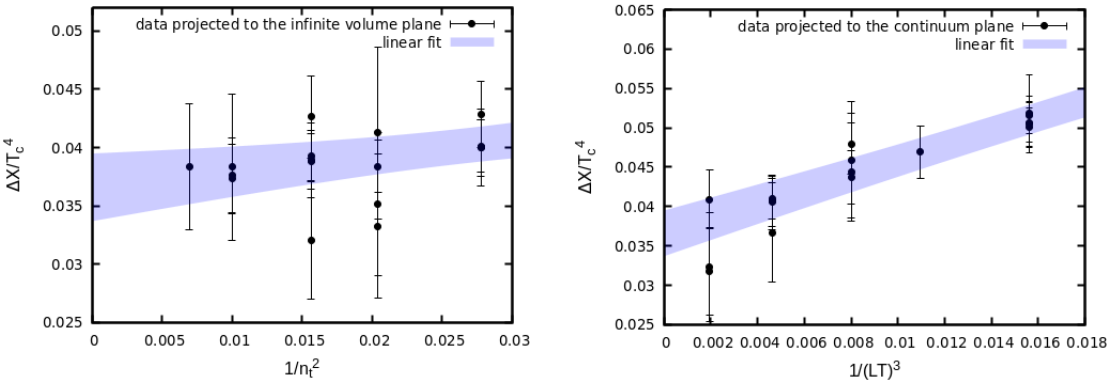

Figure 6: Discontinuity of χ at the transition temperature of ensembles listed in Tab. 1. Results of different lattices are projected onto the infinite volume plane (top) and the continuum plane (bottom). The blue bands are linear (three parameter) fits of the projected data using the same parameters as in the two dimensional fit.

from the chosen fit range include or excluding the smallest aspect ratio $LT = 4$. The other systematic varible is the choice of the fit formula for the infinite volume and continuum extrapolations. The χ^2 value of the fit was good for both a function with three parameters $f(x, y) = a + b \cdot x + c \cdot y$ ($\chi^2 = 6.3/14$ and $5.7/9$ depending on the other systematic variables) and another with four parameters $g(x, y) = a + b \cdot x + c \cdot y + d \cdot xy$ ($\chi^2 = 6/13$ and $4.6/8$), with $x = 1/N_t^2$ and $y = 1/(LT)^3$ respectively. Our result in Eq. **??** for the discontinuity of $\chi(T)$ agrees with the estimation obtained from Eq. 4.

5. Conclusion

We examined the topological features of SU(3) gauge theory via the distribution of the topological charge in the vicinity of the finite temperature deconfining transition. The two relevant observables are the toplogical susceptibility χ and the Taylor coefficient b_2 of the expansion of the free energy density at $\theta = 0$.

In Sec. 3 we examined the temperature dependence of these quantities. Since we used the renormalized topological charge, by changing the resolution $\chi(T)$ and $b_2(T)$ did not change significantly and a continuum extrapolation could be done easily (Fig. 3. We also determined these curves at different volumes. Increasing the volume at a fixed resolution resulted in a sharper fall of the susceptibility at the transition temperature (left panel in Fig. 4). This supported our expectation that the function $\chi(T)$ has a discontinuity at $T = T_c$. In Sec. 4 we determined the discontinuity $\Delta\chi$ at the transition temperature. We separated the two phases by cuting the Polyakov-loop histograms at their minima, then calculated the difference of the susceptibilities corresponding to the hot and cold phases ensemble by ensemble. Using these data we extraplated the infinite volume and continuum limit of $\Delta\chi$ (see Tab. **??**). Our result of the discontinuity is in agreement with the estimated value $\Delta\chi$ according to Eq. 4.

We analized the temperature dependence of the coefficient b_2 also in Sec. 3. As we increased the temperature toward the transition b_2 started to depart from its $T = 0$ empirical value $b_2 \approx -0.02$ and before reaching the analytical value $b_2 = -1/12$ predicted by DIGA it fell even below that at

temperatures close to the transition. This dip in $b_2(T)$ become deeper and deeper as we increased the volume (right panel in Fig. 4). This behavior can be understood through analyzing the expression of b_2 (Eq. 5). From this we can derive Eq. 8 where we can identify a volume dependent part. In the case of phase coexistence the volume dependent term is nonzero which causes a dip in $b_2(T)$ in finite volume systems near T_c. In the infinite volume limi this suggests a negative Dirac delta at the transition temperature where phase coexistence is present.

References

[1] David J. Gross, Robert D. Pisarski, and Laurence G. Yaffe. QCD and Instantons at Finite Temperature. *Rev. Mod. Phys.*, 53:43, 1981. doi: 10.1103/RevModPhys.53.43.

[2] Jaap Hoek, M. Teper, and J. Waterhouse. Topological Fluctuations and Susceptibility in SU(3) Lattice Gauge Theory. *Nucl. Phys. B*, 288:589–627, 1987. doi: 10.1016/0550-3213(87)90230-6.

[3] M. Teper. The SU(3) Topological Susceptibility at Zero and Finite Temperature: A Lattice Monte Carlo Evaluation. *Phys.Lett.*, B202:553, 1988. doi: 10.1016/0370-2693(88)91863-1.

[4] B. Alles, Massimo D'Elia, and A. Di Giacomo. Topological susceptibility in full QCD at zero and finite temperature. *Phys.Lett.*, B483:139–143, 2000. doi: 10.1016/S0370-2693(00)00556-6.

[5] B. Alles, Massimo D'Elia, and A. Di Giacomo. Topological susceptibility at zero and finite T in SU(3) Yang-Mills theory. *Nucl. Phys.*, B494:281–292, 1997. doi: 10.1016/S0550-3213(97)00205-8,10.1016/j.nuclphysb.2003.11.018. [Erratum: Nucl. Phys.B679,397(2004)].

[6] Biagio Lucini, Michael Teper, and Urs Wenger. Topology of SU(N) gauge theories at T = 0 and T = T(c). *Nucl.Phys.*, B715:461–482, 2005. doi: 10.1016/j.nuclphysb.2005.02.037.

[7] Massimo D'Elia and Francesco Negro. θ dependence of the deconfinement temperature in Yang-Mills theories. *Phys. Rev. Lett.*, 109:072001, 2012. doi: 10.1103/PhysRevLett.109.072001.

[8] Massimo D'Elia and Francesco Negro. Phase diagram of Yang-Mills theories in the presence of a θ term. *Phys.Rev.*, D88(3):034503, 2013. doi: 10.1103/PhysRevD.88.034503.

[9] S. Borsanyi, Kara R., Z. Fodor, D. A. Godzieba, P. Parotto, and D. Sexty. Precision study of the continuum SU(3) Yang-Mills theory: How to use parallel tempering to improve on supercritical slowing down for first order phase transitions. *Phys. Rev. D*, 105(7):074513, 2022. doi: 10.1103/PhysRevD.105.074513.

[10] T. Schäfer and E. V. Shuryak. Instantons in QCD. *Reviews of Modern Physics*, 70(2):323–425, apr 1998. doi: 10.1103/revmodphys.70.323. URL https://doi.org/10.1103%2Frevmodphys.70.323.

[11] Reka A. Vig and Tamas G. Kovacs. Ideal topological gas in the high temperature phase of SU(3) gauge theory. *Phys. Rev. D*, 103(11):114510, 2021. doi: 10.1103/PhysRevD.103.114510.

[12] Claudio Bonati, Massimo D'Elia, Haralambos Panagopoulos, and Ettore Vicari. Change of θ Dependence in 4D SU(N) Gauge Theories Across the Deconfinement Transition. *Phys. Rev. Lett.*, 110(25):252003, 2013. doi: 10.1103/PhysRevLett.110.252003.

[13] Claudio Bonati, Massimo D'Elia, and Aurora Scapellato. θ dependence in $SU(3)$ Yang-Mills theory from analytic continuation. *Phys. Rev.*, D93(2):025028, 2016. doi: 10.1103/PhysRevD.93.025028.

[14] Haralambos Panagopoulos and Ettore Vicari. The 4D SU(3) gauge theory with an imaginary θ term. *JHEP*, 11:119, 2011. doi: 10.1007/JHEP11(2011)119.

[15] Marco Cè, Cristian Consonni, Georg P. Engel, and Leonardo Giusti. Non-Gaussianities in the topological charge distribution of the SU(3) Yang–Mills theory. *Phys. Rev. D*, 92(7):074502, 2015. doi: 10.1103/PhysRevD.92.074502.

[16] Massimo D'Elia. Field theoretical approach to the study of theta dependence in Yang-Mills theories on the lattice. *Nucl. Phys. B*, 661:139–152, 2003. doi: 10.1016/S0550-3213(03)00311-0.

[17] Leonardo Giusti, Silvano Petrarca, and Bruno Taglienti. Theta dependence of the vacuum energy in the SU(3) gauge theory from the lattice. *Phys. Rev. D*, 76:094510, 2007. doi: 10.1103/PhysRevD.76.094510.

[18] Guy D. Moore. Improved Hamiltonian for Minkowski Yang-Mills theory. *Nucl. Phys. B*, 480:689–728, 1996. doi: 10.1016/S0550-3213(96)00497-X.

[19] Philippe de Forcrand, Margarita Garcia Perez, and Ion-Olimpiu Stamatescu. Topology of the SU(2) vacuum: A Lattice study using improved cooling. *Nucl. Phys. B*, 499:409–449, 1997. doi: 10.1016/S0550-3213(97)00275-7.

[20] Sundance O. Bilson-Thompson, Derek B. Leinweber, and Anthony G. Williams. Highly improved lattice field strength tensor. *Annals Phys.*, 304:1–21, 2003. doi: 10.1016/S0003-4916(03)00009-5.

[21] Martin Luscher. Properties and uses of the Wilson flow in lattice QCD. *JHEP*, 1008:071, 2010. doi: 10.1007/JHEP08(2010)071.

[22] Stephan Dürr, Zoltan Fodor, Christian Hoelbling, and Thorsten Kurth. Precision study of the SU(3) topological susceptibility in the continuum. *Journal of High Energy Physics*, 2007(04):055–055, apr 2007. doi: 10.1088/1126-6708/2007/04/055. URL https://doi.org/10.1088%2F1126-6708%2F2007%2F04%2F055.